Available online at www.sciencedirect.com
SCIENCE DIRECT®
Journal of Molecular Spectroscopy 221 (2003) 250–260
Journal of MOLECULAR SPECTROSCOPY
www.elsevier.com/locate/jms

High resolution fourier transform spectrum of PD_3 in the region of the stretching overtone bands $2\nu_1$ and $\nu_1 + \nu_3$ ☆

O.N. Ulenikov,[a,b,*] Yu.B. Yuhnik,[a,b] E.S. Bekhtereva,[a,b] N.E. Tyabaeva,[a,b] H. Bürger,[c] W. Jerzembeck,[c] and L. Fusina[d]

[a] *Laboratory of Molecular Spectroscopy, Physics Department, Tomsk State University, Lenin Avenue 36, Tomsk 634050, Russia*
[b] *Institute of Atmospheric Optics SB RAN, Tomsk 634055, Russia*
[c] *Anorganische Chemie, FB 9, Bergische Universität, Wuppertal D-42097, Germany*
[d] *Dipartimento di Chimica Fisica e Inorganica, Università di Bologna, Viale Risorgimento 4, Bologna I-40136, Italy*

Received 9 May 2003; in revised form 14 July 2003

Abstract

The infrared spectrum of the PD_3 molecule has been measured in the region of the first stretching overtone bands on a Fourier transform spectrometer with a resolution of $0.0068\,cm^{-1}$ and analyzed for the first time. More than 800 transitions with $J^{max} = 15$ have been assigned to the bands $2\nu_1$ and $\nu_1 + \nu_3$. An effective Hamiltonian was used which takes into account both the presence of resonance interactions between the states (2 0 0 0) and (1 0 1 0), and interactions of these with the third stretching vibrational state of the $v = 2$ polyad, (0 0 2 0). A set of 44 spectroscopic parameters is obtained from the fit. This reproduces the 305 initial "experimental" upper rovibrational energies with an rms $= 0.0015\,cm^{-1}$.

Keywords: Vibration–rotation spectra; PD_3 molecule; Stretching overtones; Spectroscopic parameters

1. Introduction

Whenever it is desirable to obtain as complete as possible spectroscopic information on a target molecule, the study of isotopic varieties of this molecule is an efficient means to gather valuable additional information, in particular of peculiar intramolecular dynamics. The larger the mass ratio of the isotopically labelled variety with regard to the reference "mother" molecule is, the more pronounced are the apparent isotopic effects on the spectrum and the rovibrational energy pattern. The greater the variety of isotopic substitution, the more effects can be detected and studied in detail. Accordingly, the study of deuterated species of a molecule is the most efficient because the ratio $(m_D - m_H)/m_H$ is the largest one for stable isotopes. Moreover, deuterated species are usually available by feasible synthetic routes.

In this contribution we present the results of the high resolution spectroscopic study of the first stretching overtones of the totally deuterated species of the phosphine molecule, PD_3. This investigation on PD_3 follows a series of high resolution studies on the asymmetric rotors PH_2D and PHD_2 (see [1,2] for leading relevant information). Interest in the different phosphine species originates both in application aspects, for example, planetology and astrophysics [3–5], and reasons of basic molecular physics. Thus, the phosphine molecule is one of the lightest tetraatomic symmetric tops. It is therefore to be expected that perturbational effects will be particularly clearly pronounced in PH_3 and its deuterated varieties.

One of such isotope-dependent phenomena is the extent to which local mode properties occurring in the XH_n $(n = 2, 3, 4)$ molecules vary, or persist, upon deuteration. It is, in particular, interesting to assess local

☆ Supplementary data for this article are available on ScienceDirect.

* Corresponding author. Fax: +7-49-20-24-39-2581.
E-mail address: Ulenikov@phys.tsu.ru (O.N. Ulenikov).

0022-2852/$ - see front matter © 2003 Elsevier Inc. All rights reserved.
doi:10.1016/S0022-2852(03)00224-8

mode phenomena in XD_n molecules both in comparison with the XH_n molecules, and in dependence of increasing X–D-stretching excitation. For this purpose, high resolution infrared studies of stretching overtones are interesting and timely. Inspection of relevant literature reveals that former stretching fundamental and overtone studies emphasizing local mode effects are restricted to pairs of asymmetric top molecules, XH_2/XD_2 (H_2S/D_2S [6,7], H_2Se/D_2Se [8]), and spherical tops, XH_4/XD_4 (SiH_4/SiD_4 [9,10], GeH_4/GeD_4 [11,12], and SnH_4/SnD_4 [13]).[1] No such studies on XH_3/XD_3 molecules have come yet to our attention, reported studies on the ν_1/ν_3 fundamental bands of PD_3 being only a first step in that direction [14,15].

The infrared spectra of the PD_3 molecule in the regions of the fundamental vibrations, ν_1/ν_3 [15] and ν_2/ν_4 [16], and in the far-infrared [17] have been studied recently. A discussion on the ground state of PD_3 including new pure rotational data in the millimeter-wave (MMW) and THz ranges as well as in the far-IR range, and in addition ground state combination differences (GSCD), including such with $\Delta K \neq 0$ obtained from the ν_1/ν_3 and ν_2/ν_4 bands, has been carried out [17]. As to the first stretching overtone bands, these have never been investigated before, therefore their Fourier transform spectra in the region 3200–3450 cm^{-1} were recorded with a resolution of 0.0068 cm^{-1} and analysed in our present study. The respective experimental details are given in Section 2. Section 3 presents briefly the Hamiltonian used in the fit of the rotational–vibrational energies extracted from the experimental data. Assignments of the recorded transitions are gathered in Section 4. Sections 5 and 6 give the prediction of spectroscopic parameters by a local mode model and the results of the fit of derived upper state energies, respectively. In Section 7 we will discuss the problem of local mode behaviour of the $2\nu_1/\nu_1+\nu_3$ overtones in comparison to that of the ν_1/ν_3 fundamentals, and in Section 8 we will draw a conclusion.

2. Experimental details

PD_3 was prepared as described earlier [17]. The degree of deuteration was rather high but in order to identify weak absorptions by PHD_2 and PH_2D we made use of a spectrum mostly revealing absorptions of the latter species and recorded under very similar conditions.

For the recording of the spectra a Bruker 120 HR interferometer was used. This was equipped with a halogen source, a KBr beam splitter, and an InSb detector. An optical band filter limited the spectral range to 2900–4000 cm^{-1}. The resolution (1/maximum optical path difference) was 6.8×10^{-3} cm^{-1}, and trapezoidal apodization was applied. The optical path length of a White-type cell was adjusted to 16 m, and a pressure of 300 Pa chosen. In total 750 scans were collected. Calibration was done using H_2O lines in the 3800 cm^{-1} region as quoted in [18]. Wavenumber precision is ca. 0.3×10^{-3} cm^{-1}, wavenumber accuracy better than 1×10^{-3} cm^{-1}.

3. Theoretical background

Like PH_3, PD_3 is an oblate symmetric top with a DPD bond angle close to 90°. Its stretching fundamental bands ν_1 and ν_3 are close to each other with band centers at 1682.12 and 1693.35 cm^{-1}, respectively [15]. They are located at about two times higher wavenumbers than the bending fundamentals ν_2 and ν_4 (728.29 and 803.14 cm^{-1}, respectively [16]). Since PD_3 is a light molecule, with large rotational parameters ($B_0 = 2.3173068$ cm^{-1}, $C_0 = 1.9671788$ cm^{-1} [17]), it is to be expected that close-lying vibrational levels will undergo strong vibrational interactions both of Fermi and Coriolis type. Moreover, intravibrational resonances will be prominent in accordance with the dense pattern of rotational energy levels.

In the present study, we therefore adopt a Hamiltonian model derived previously [19] on the basis of the symmetry properties of the molecule. This model allows to take into account any kind of effects and interactions appearing in every polyads. This Hamiltonian has the form of the effective operator

$$H^{v.-r.} = \sum_{v,v'} H^{vv'}, \tag{1}$$

where the summation extends to all vibrational states of a polyad. The diagonal operators H^{vv} describe rotational structures of corresponding vibrational states. The nondiagonal operators $H^{vv'}$ ($v \neq v'$) describe resonance interactions between the states $|v\rangle$ and $|v'\rangle$. In the case of symmetric vibrational states (A_1 symmetry), the $H^{A_1A_1}$ operators have the form

$$\begin{aligned} H^{A_1A_1} = |A_1\rangle\langle A_1|\{&E^a + B^a(J_x^2+J_y^2) + C^aJ_z^2 - D_J^aJ^4 \\ &- D_{JK}^aJ^2J_z^2 - D_K^aJ_z^4 + H_J^aJ^6 + H_{JK}^aJ^4J_z^2 \\ &+ H_{KJ}^aJ^2J_z^4 + H_K^aJ_z^6 + L_J^aJ^8 + L_{JJK}^aJ^6J_z^2 + \cdots \\ &+ [(\epsilon'^aJ_z + \epsilon_J'^aJ_zJ^2 + \epsilon_K'^aJ_z^3 + \cdots), \\ &(J_+^3 + J_-^3)]_+ + h'^a(J_+^6 + J_-^6) + \cdots\} \end{aligned} \tag{2}$$

[1] We mention here only one or two references related to the deuterated species. The numerous references dealing with the "mother" species are not mentioned for brevity reasons.

Here $B^a, C^a, D^a_J, D^a_{JK}, D^a_K, \ldots$ are the rotational and centrifugal distortion parameters, respectively. Operators $(J^3_+ + J^3_-)$ connect rotational states $|JK\rangle$ and $|JK'\rangle$ with different values of the quantum numbers K, namely $\Delta K = K - K' = \pm 3$. They account, in particular, for the A_1/A_2 splittings of $K = 3$ levels. Parameters ϵ'^a_J and ϵ'^a_K describe the J and K dependences of the main ϵ'^a parameter. The expression $[\ldots,\ldots]_+$ denotes an anticommutator.

For doubly degenerate vibrational states (E symmetry) the H^{EE} operator is

$$H^{EE} = H^{EE}_1 + H^{EE}_2 + H^{EE}_3, \tag{3}$$

where

$$\begin{aligned} H^{EE}_1 = {} & (|E_1\rangle\langle E_1| + |E_2\rangle\langle E_2|)\{E^e + B^e(J^2_x + J^2_y) \\ & + C^e J^2_z - D^e_J J^4 - D^e_{JK} J^2 J^2_z - D^e_K J^4_z + H^e_J J^6 \\ & + H^e_{JK} J^4 J^2_z + H^e_{KJ} J^2 J^4_z + H^e_K J^6_z + L^e_J J^8 + L^e_{JJK} J^6 J^2_z \\ & + \cdots + [(\epsilon'^e J_z + \epsilon'^e_J J_z J^2 + \epsilon'^e_K J^3_z + \cdots), (J^3_+ + J^3_-)]_+ \end{aligned} \tag{4}$$

$$\begin{aligned} H^{EE}_2 = {} & (|E_1\rangle\langle E_2| - |E_2\rangle\langle E_1|)\{2(C\zeta)J_z + \eta_J J_z J^2 \\ & + \eta_K J^3_z + \eta_{JJ} J_z J^4 + \eta_{JK} J^3_z J^2 + \eta_{KK} J^5_z \\ & + \eta_{JJJ} J_z J^6 + \eta_{JJK} J^3_z J^4 + \eta_{JKK} J^5_z J^2 + \eta_{KKK} J^7_z + \cdots\}, \end{aligned} \tag{5}$$

and

$$\begin{aligned} H^{EE}_3 = {} & (|E_2\rangle\langle E_2| - |E_1\rangle\langle E_1|)\{[\mathrm{i}A, (J_+ - J_-)]_+ \\ & + [B, (J_+ + J_-)]_+ + [C, (J^2_+ + J^2_-)]_+ \\ & + [\mathrm{i}D, (J^2_- - J^2_+)]_+ + [F, (J^4_+ + J^4_-)]_+ \\ & + [\mathrm{i}G, (J^4_- - J^4_+)]_+\} + (|E_1\rangle\langle E_2| + |E_2\rangle\langle E_1|) \\ & \times \{[A, (J_+ + J_-)]_+ + [\mathrm{i}B, (J_- - J_+)]_+ \\ & + [\mathrm{i}C, (J^2_+ - J^2_-)]_+ + [D, (J^2_+ + J^2_-)]_+ \\ & + [\mathrm{i}F, (J^4_+ - J^4_-)]_+ + [G, (J^4_+ + J^4_-)]_+\}, \end{aligned} \tag{6}$$

$$\begin{aligned} A &= \frac{1}{2}\alpha + \frac{1}{2}\alpha_J J^2 + \alpha_K J^2_z + \cdots + \alpha_{KK} J^4_z + \cdots, \\ B &= \beta J_z + \beta_J J_z J^2 + \beta_K J^3_z + \cdots, \\ C &= \frac{1}{2}\gamma + \frac{1}{2}\gamma_J J^2 + \gamma_K J^2_z + \frac{1}{2}\gamma_{JJ} J^4 + \gamma_{JK} J^2 J^2_z + \cdots, \\ D &= \delta J_z + \delta_J J_z J^2 + \delta_K J^3_z + \delta_{JJ} J_z J^4 + \delta_{JK} J^2 J^3_z + \cdots, \\ F &= \frac{1}{2}\kappa + \frac{1}{2}\kappa_J J^2_z + \kappa_K J^2_z + \frac{1}{2}\kappa_{JJ} J^4 + \kappa_{JK} J^2 J^2_z + \cdots, \\ G &= \theta J_z + \theta_J J_z J^2 + \theta_K J^3_z. \end{aligned} \tag{7}$$

In Eq. (4) the $E^e, B^e, \ldots, \epsilon'^e$ parameters have the same meaning as the corresponding ones in Eq. (2) with only one exception: although operators $(J^3_+ + J^3_-)$ connect rotational states $|JK\rangle$ and $|JK'\rangle$ with $\Delta K = K - K' = \pm 3$, they do not split A_1/A_2 levels. The operator H^{EE}_2 describes the $k - l$ splittings; other type operators, $(J^n_+ \pm J^n_-)$, connect rotational states $|JK\rangle$ and $|JK'\rangle$ where $\Delta K = K - K' = \pm n$. Of these, the operators with $n = 2m$ provide the $A_1 - A_2$ splittings of energy levels with $K = m$.

Resonance interaction parameters can be divided into two types:

(1) Fermi-type ones which connect vibrational states of the same symmetry. In this case, the corresponding $H^{v\Gamma,v'\Gamma'}$ operators have the form

$$\begin{aligned} H^{vA_1,v'A_1} = {} & |vA_1\rangle\langle v'A_1|\{F^{v-v'}_0 + F^{v-v'}_J(J^2_x + J^2_y) \\ & + F^{v-v'}_K J^2_z + F^{v-v'}_{JJ} J^4 + F^{v-v'}_{JK} J^2 J^2_z \\ & + F^{v-v'}_{KK} J^4_z + F^{v-v'}_{JJJ} J^6 + F^{v-v'}_{JJK} J^4 J^2_z \\ & + F^{v-v'}_{JKK} J^2 J^4_z + \cdots + F^{v-v'}_{JJJJ} J^8 \\ & + F^{v-v'}_{JJJK} J^6 J^2_z + \cdots + [(\tilde{\epsilon}'^a J_z + \tilde{\epsilon}'^a_J J_z J^2 \\ & + \tilde{\epsilon}'^a_K J^3_z + \cdots), (J^3_+ + J^3_-)]_+\} \end{aligned} \tag{8}$$

and

$$H^{vE,v'E} = H^{vE,v'E}_1 + H^{vE,v'E}_2 + H^{vE,v'E}_3, \tag{9}$$

$$\begin{aligned} H^{vE,v'E}_1 = {} & (|E_1\rangle\langle E_1| + |E_2\rangle\langle E_2|)\{F^{v-v'}_0 + F^{v-v'}_J(J^2_x + J^2_y) \\ & + F^{v-v'}_K J^2_z + F^{v-v'}_{JJ} J^4 + F^{v-v'}_{JK} J^2 J^2_z \\ & + F^{v-v'}_{KK} J^4_z + F^{v-v'}_{JJJ} J^6 + F^{v-v'}_{JJK} J^4 J^2_z \\ & + F^{v-v'}_{JKK} J^2 J^4_z + \cdots + F^{v-v'}_{JJJJ} J^8 \\ & + F^{v-v'}_{JJJK} J^6 J^2_z + \cdots + [(\tilde{\epsilon}'^e J_z + \tilde{\epsilon}'^e_J J_z J^2 \\ & + \tilde{\epsilon}'^e_K J^3_z + \cdots), (J^3_+ + J^3_-)]_+\} \end{aligned} \tag{10}$$

$$\begin{aligned} H^{vE,v'E}_2 = {} & (|E_1\rangle\langle E_2| - |E_2\rangle\langle E_1|)\{2(\widetilde{C\zeta})J_z \\ & + \tilde{\eta}_J J_z J^2 + \tilde{\eta}_K J^3_z + \tilde{\eta}_{JJ} J_z J^4 + \tilde{\eta}_{JK} J^3_z J^2 \\ & + \tilde{\eta}_{KK} J^5_z + \tilde{\eta}_{JJJ} J_z J^6 + \tilde{\eta}_{JJK} J^3_z J^4 \\ & + \tilde{\eta}_{JKK} J^5_z J^2 + \tilde{\eta}_{KKK} J^7_z + \cdots\}, \end{aligned} \tag{11}$$

$$\begin{aligned} H^{vE,v'E}_3 = {} & (|E_2\rangle\langle E_2| - |E_1\rangle\langle E_1|)\{[\mathrm{i}\tilde{A}, (J_+ - J_-)]_+ \\ & + [\tilde{B}, (J_+ + J_-)]_+ + [\tilde{C}, (J^2_+ + J^2_-)]_+ \\ & + [\mathrm{i}\tilde{D}, (J^2_- - J^2_+)]_+ + [\tilde{F}, (J^4_+ + J^4_-)]_+ \\ & + [\mathrm{i}\tilde{G}, (J^4_- - J^4_+)]_+\} + (|E_1\rangle\langle E_2| + |E_2\rangle\langle E_1|) \\ & \{[\tilde{A}, (J_+ + J_-)]_+ + [\mathrm{i}\tilde{B}, (J_- - J_+)]_+ \\ & + [\mathrm{i}\tilde{C}, (J^2_+ - J^2_-)]_+ + [\tilde{D}, (J^2_+ + J^2_-)]_+ \\ & + [\mathrm{i}\tilde{F}, (J^4_+ - J^4_-)]_+ + [\tilde{G}, (J^4_+ + J^4_-)]_+\}. \end{aligned} \tag{12}$$

Here the operators $\tilde{A}, \tilde{B}, \ldots$, can be derived from Eq. (7) by replacing the parameters $\alpha, \beta, \ldots$ by parameters $\tilde{\alpha}, \tilde{\beta}, \ldots$

(2) Coriolis-type resonance operators which connect vibrational states of different symmetries, A_1 and E. In this case,

$$
\begin{aligned}
H^{vA_1,v'E} = {} & |A_1\rangle\langle E_1|\{[\mathrm{i}A^*,(J_+ - J_-)]_+ + [B^*,(J_+ + J_-)]_+ \\
& + [C^*,(J_+^2 + J_-^2)]_+ + [\mathrm{i}D^*,(J_-^2 - J_+^2)]_+ \\
& + [F^*,(J_+^4 + J_-^4)]_+ + [\mathrm{i}G^*,(J_-^4 - J_+^4)]_+\} \\
& + |A_1\rangle\langle E_2|\{[A^*,(J_+ + J_-)]_+ \\
& + [\mathrm{i}B^*,(J_- - J_+)]_+ + [\mathrm{i}C^*,(J_+^2 - J_-^2)]_+ \\
& + [D^*,(J_+^2 + J_-^2)]_+ + [\mathrm{i}F^*,(J_+^4 - J_-^4)]_+ \\
& + [G^*,(J_+^4 + J_-^4)]_+\}. \qquad (13)
\end{aligned}
$$

As in the case of the Fermi type interaction, the operators $A^*, B^*, \ldots$, can be derived from Eq. (7) by replacing the parameters $\alpha, \beta, \ldots$ by $\alpha^*, \beta^*, \ldots$

4. Description and assignment of the spectrum

In the recorded spectral region three stretching overtone bands are expected, $2\nu_1$, $\nu_1 + \nu_3$, and $2\nu_3$. The two bands $2\nu_1$ and $\nu_1 + \nu_3$ are close to each other, and there is both extended overlap of these bands and strong resonance interactions between respective upper rovibrational levels. No transitions belonging to $2\nu_3$ were identified because the intensity of the band is very low.

The separation between the deperturbed centers of the $2\nu_1$ and $\nu_1 + \nu_3$ bands is only $2.8\,\mathrm{cm}^{-1}$. So, in the overview spectrum (see Fig. 1), one can see only a single strong Q-branch feature near $3330\,\mathrm{cm}^{-1}$ which results from the overlap of three types of transitions, namely ${}^QQ_K(J)$ of $2\nu_1$, and ${}^PQ_K(J)$ and ${}^RQ_K(J)$ of $\nu_1 + \nu_3$. These branches reveal similar intensities. The feature associated with the Q-branches is red degraded.

The regular J-cluster structure of the R-branch of the $2\nu_1$ band is also quite prominent and visible in the higher wavenumber region. The P-branch region is not that regularly clustered because it overlaps with the R- and Q-branches of a perturber band. This additional band, centered near $3280\,\mathrm{cm}^{-1}$, is only slightly weaker, and supposedly due to $\nu_1 + 2\nu_4$ and $\nu_3 + 2\nu_4$, see Fig. 1. The combination levels $\nu_1 + 2\nu_4(A_1 + E)$ and $\nu_3 + 2\nu_4$ $(A_1 + A_2 + 2E)$ are not dark states but are reached by transitions which apparently borrow intensity from the $2\nu_1$ and/or $\nu_1 + \nu_3$ vibrational bands via anharmonic interactions. Although these additional bands are not considered in the present study, effects on wavenumbers of $2\nu_1$ and $\nu_1 + \nu_3$ may not be negligible and may be of influence on the parameters of the (2 0 0 0) and (1 0 1 0) states.

The $2\nu_1$ band illustrated in some detail in Fig. 2 is characterized by a strong R-branch while the P- and Q-branches are weak. However, the series of the ${}^QQ_{K=J}(J)$ transitions is prominent and their strength comparable with the strongest ${}^QR_K(J)$ lines. The intensity of ${}^QQ_K(J)$ transitions decreases both as the J value for a given K increases and the K value for a given J increases. In the ${}^QQ_{K=J}(J)$ transitions, for our experimental conditions, peaks had a minimum transmittance of about 60–65% while ${}^QQ_{K=J-2}(J)$ lines are already to weak to be clearly observed.

The Q-branches of the $2\nu_1$ band are red degraded and visible from 3325 to $3333\,\mathrm{cm}^{-1}$, and extend up to $J^{\max} = 14$. The R-branch is J-clustered, and lines of such clusters are red degraded for large K. The low-K components are irregularly displaced from the cluster origins in correspondence to the Coriolis interaction with $\nu_1 + \nu_3$ involving K, $(k - l)$ level crossing. Clusters up to $J = 12$ are clearly visually discernible in the spectrum. The A_1/A_2 splittings of $K = 3$ transitions are small and resolved for $J \geqslant 9$. The P-branch of the $2\nu_1$ band is weak, and no prominent features are discernible.

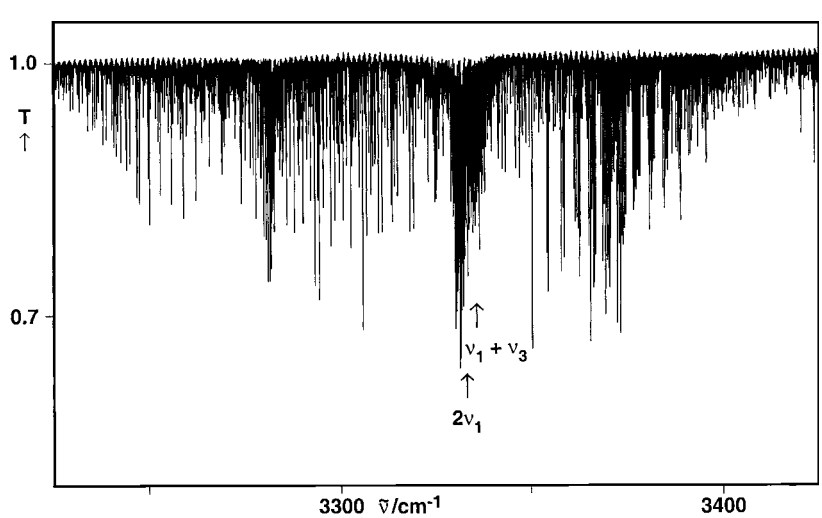

Fig. 1. Survey spectrum of the $2\nu_1$ and $\nu_1 + \nu_3$ bands of PD_3. Deperturbed band centers are denoted. Note the single strong Q-branches feature near $3330\,\mathrm{cm}^{-1}$ which results from the overlap of ${}^QQ$-branches of $2\nu_1$ and of ${}^PQ$- and/or ${}^RQ$-branches of $\nu_1 + \nu_3$. Note furthermore the Q-branches of $\nu_1 + 2\nu_4$ and $\nu_3 + 2\nu_4$ near $3280\,\mathrm{cm}^{-1}$.

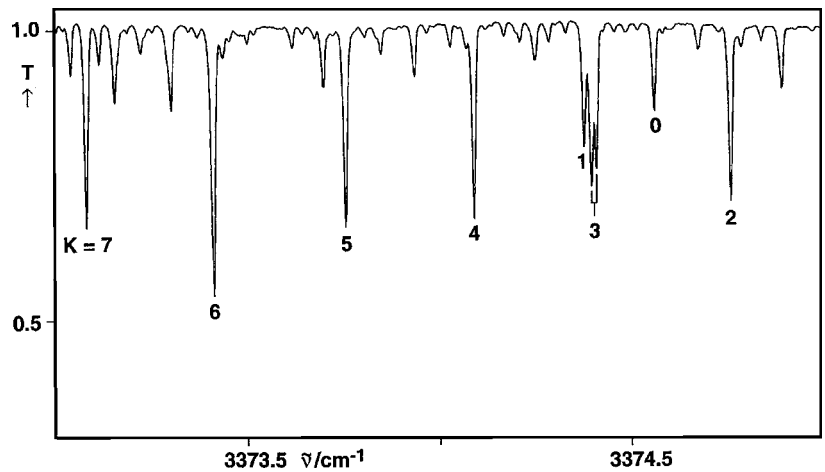

Fig. 2. The $^{Q}R_K(9)$ cluster of the $2\nu_1$ band of PD_3. The K assignment is given.

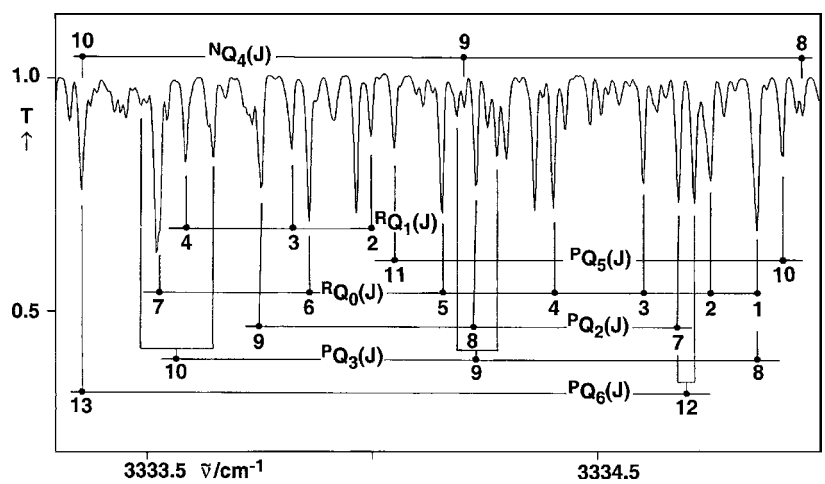

Fig. 3. Detail of the Q-branches region of the $\nu_1 + \nu_3$ band of PD_3. Some assignments of ^{P}Q- and ^{R}Q-branches are given. Note the forbidden, but perturbation-allowed $^{N}Q_4$ transitions denoted on top of the trace. The splitting of the $^{P}Q_6(12)$ transition of $\nu_1 + \nu_3$ due to resonance interactions with $2\nu_1$ can be seen.

The $\nu_1 + \nu_3$ band, a small part of which is illustrated in Fig. 3, is characterized by the strong $^{P}Q_K(J)$, and $^{R}Q_K(J)$ branches located in the 3330–3337 cm^{-1} region. The $^{R}R_K(J)$ transitions are quite strong for $K = 0$–2. However, the line strengths are rapidly decreasing both with increasing J and K quantum numbers. The $^{P}R_K(J)$ transitions are very weak.

In general, $\Delta J = +1$ transitions of the $\nu_1 + \nu_3$ band are considerably weaker than the corresponding ones of the $2\nu_1$ band. There is no systematic feature visible which would enable any direct assignment to be made.

The $^{R}P_K(J)$- and $^{P}P_K(J)$-type transitions in the P-branch are comparable in strength both among themselves, and with the Q-type transitions. The high J P-branch clusters apparently reveal a K-degradation to the blue.

In Fig. 3 a local splitting of the $^{P}Q_6(12)$ transition can be seen which is caused by strong resonance interactions with the $2\nu_1$ level. For the same reason, numerous "forbidden" transitions can be assigned in the experimental spectrum, see below. One set of such "forbidden" transitions in the $2\nu_1$ band, $^{N}Q_4(J)$ is also shown in Fig. 3.

Since the $\nu_1 + \nu_3$ band is of perpendicular type, while the $2\nu_1$ band is a parallel one, the interactions between the excited levels are of Coriolis type and can be described by the operator $H^{vA_1 v'E}$, Eq. (13). In accordance with the symmetry, the selection rules for the strongest "allowed" transitions are

$$\Delta J = 0, \pm 1;\ \ \Delta K = 0;\ \ E \to E,\ A_1 \leftrightarrow A_2 \quad \text{if } K \neq 0,$$

$$\Delta J = \pm 1;\ \ \Delta K = 0;\ \ A_1 \leftrightarrow A_2 \quad \text{if } K = 0,$$

for the parallel band $2\nu_1$ and

$$\Delta J = 0, \pm 1;\ \ \Delta K = \pm 1;\ \ E \to E,\ A_1 \leftrightarrow A_2,$$

for the perpendicular band $\nu_1 + \nu_3$.

Table 1
Experimental rovibrational term values for the (2000,A_1) vibrational state of PD_3 (in cm^{-1})[a]

J	K	Γ	E	Δ	δ
1			2	3	4
0	0	A_1	3332.5414		5
1	0	A_2	3337.1087	1	5
1	1	E	3336.7747	3	3
2	0	A_1	3346.2398	3	−4
2	1	E	3345.9046	2	3
2	2	E	9344.9058	3	0
3	0	A_2	3359.9350		34
3	1	E	3359.5890	4	7
3	2	E	3358.5748	3	−6
3	3	A_1	3356.9367	4	−5
3	3	A_2	3956.9321	4	−5
4	0	A_1	3378.1057	0	2
4	1	E	3377.8151	10	−2
4	2	E	3376.7189	4	−5
9	3	A_3	3375.0144	5	−4
4	4	A_2	3370.0144	5	−5
4	4	E	3372.8538	15	−12
5	0	A_2	3400.9636	2	7
5	1	E	3700.5745	2	0
5	2	E	3399.5768	5	−2
5	3	A_1	3397.5213	6	−11
5	0	A_2	3397.7214	3	−7
5	2	E	3394.4804		4
5	5	E	3392.6685	2	−12
4	0	A_1	3526.2812	6	−7
6	1	E	3427.8765	2	3
6	2	E	3426.1053	2	−3
1	5	A_1	2424.9977	2	3
6	3	A_2	3424.9977	2	−7
6	4	E	3422.6517	3	0
6	5	E	8468.6810	4	19
6	4	A	3410.3765	6	1
7	0	A_2	0460.1363	2	−1
7	1	E	3459.7023	5	5
7	2	E	3458.7822	1	−1
7	3	A_1	3456.8295	11	2
7	3	A_2	3456.8295	11	27
7	4	E	3454.0812	6	1
7	8	E	2480.5396	8	−2
7	6	A	5446.2519		−20
7	7	E	3443.9756	2	7
8	7	A_1	3496.5199	3	−4
6	1	E	3436.1538	1	8
8	2	E	3495.2041	3	4
8	3	A_1	3193.2055	11	32
8	3	A_5	3493.2455	11	−94
8	4	E	3490.4588	10	4
8	5	E	7351.9449	4	4
8	6	A	3482.6914	6	0
8	7	E	0479.7253	8	−3
8	8	E	3375.4706	6	11
9	0	A_2	3587.4304	3	−6
8	1	E	3137.9263	8	2
9	2	E	3536.1675	5	5
1	1	A_1	3535.1282		31
9	3	A_2	3534.1499		46
9	4	E	3534.3782	7	15
9	5	E	3527.8886	7	−9
9	6	A	3523.6718	6	−10
9	7	E	3518.7489	4	78

Table 1 (*continued*)

J	K	Γ	E	Δ	δ
1			2	3	4
9	8	E	3513.1331	16	19
9	9	A	3510.8688	12	51
80	0	A_1	3582.8477	2	−9
10	1	E	3581.3188	40	6
10	8	E	3581.6606	3	6
10	4	A_1	3572.5547	8	28
10	3	A_2	3579.5789	12	18
10	4	E	3576.8308	1	8
10	5	E	3573.3674		−25
10	6	A	3569.1921	3	−9
10	7	E	3564.3230		95
20	8	E	3558.7470	8	−1
10	10	E	3550.1827	5	13
11	0	A_2	3632.8607	2	−6
11	5	E	3632.2285	10	−7
11	2	E	3331.6793	3	0
21	3	A_6	3629.2567	4	−9
11	3	A_5	3629.5358	6	27
11	4	E	3622.8104		−24
11	5	E	3623.3800	20	−34
11	6	A	3689.2549	3	31
91	7	E	3614.4227	10	−25
12	0	A_1	3687.4476	6	−6
12	1	E	3686.6640	5	−12
12	2	E	0686.2007	4	9
12	3	A_1	3684.0258	7	30
12	3	A_2	3684.0184	5	−27
12	4	E	2681.3135	11	−33
52	5	E	3677.9287	10	13
16	6	A	3673.8486	42	5
93	0	A_2	9746.6621	6	2
13	1	E	3745.4399	5	−24
14	2	E	3745.2301		47
13	3	A_8	3743.0809	11	10
13	3	A_2	3743.0315	9	52
13	5	E	3846.9990	11	10
14	1	E	3809.1774	3	16
14	4	E	3803.8780	7	−11

[a] Γ is the symmetry of a rovibrational state; Δ is the experimental uncertainty of the energy value, equal to one standard deviation in units of $10^{-4}\,cm^{-1}$; δ is the difference $E^{exp.} - E^{calc.}$, in units of $10^{-4}\,cm^{-1}$; Δ is not quoted when the energy value was obtained from only one transition.

Assignments of lines of the recorded spectrum were made on the basis of the ground state combination differences method, and the ground state energies were taken from [17]. More than 800 transitions were assigned to the $2\nu_1$ and $\nu_1 + \nu_3$ bands. Upper "experimental" rovibrational energies and their uncertainties Δ, for both vibrational bands, were determined from transitions reaching the same upper state and are presented in columns 2 and 3 of Tables 1 and 2 in units of cm^{-1} and $10^{-4}\,cm^{-1}$, respectively. No Δ value is quoted when the upper energy value was obtained from only one transition.

Table 2
Experimental rovibrational term values for the (1010,E) vibrational state of PD_3 (in cm^{-1})[a]

J	K	Γ	E	Δ	δ
1			2	3	4
0	0	E	3335.3091		9
1	1	A_1	3339.4927		5
1	1	A_2	3339.4669	2	−3
1	0	E	3339.8776	6	1
1	1	E	3339.6063	4	−5
2	2	E	3347.5569	2	−1
2	1	A_1	3348.5855	1	−6
2	1	A_2	3348.6584	6	−14
2	0	E	3349.0163	9	−1
2	1	E	3348.7420	5	−1
2	2	A_1	3347.8042	6	−3
2	2	A_2	3347.8042	6	5
3	3	E	3359.5573	2	4
3	2	E	3361.2813	1	−1
3	1	A_1	3362.4102	3	1
3	1	A_2	3362.2647	2	−7
3	0	E	3362.7258	3	2
3	1	E	3362.4452	2	−1
3	2	A_1	3361.5024	8	12
3	2	A_2	3361.5024	8	−26
3	3	E	3359.9048	6	2
4	4	A	3375.5819	3	4
4	3	E	3377.8923	5	3
4	2	E	3379.5766	2	0
4	1	A_1	3380.5060	1	−9
4	1	A_2	3380.7409	7	15
4	0	E	3381.0066	2	4
4	1	E	3380.7168	17	−1
4	2	A_1	3379.7738	3	5
4	2	A_2	3379.7628	6	5
4	3	E	3378.1783	3	−2
4	4	E	3375.8875	5	7
5	5	E	3395.8705	3	−7
5	4	A	3398.5708	2	−3
5	3	E	3400.8019	2	4
5	2	E	3402.4387	2	1
5	1	A_1	3403.6495	4	0
5	1	A_2	3403.3146	7	−3
5	0	E	3403.8600	3	8
5	1	E	3403.5576	3	−5
5	2	A_1	3402.5860	3	2
5	2	A_2	3402.6071	3	8
5	3	E	3401.0234	2	−1
5	4	E	3398.6916	8	6
5	5	A	3395.7761		4
6	6	E	3420.2162	9	−8
6	5	E	3423.4342	10	−8
6	4	A_1	3426.1113	3	7
6	4	A_2	3426.1113	3	−9
6	3	E	3428.2798	3	2
6	2	E	3429.8629	2	2
6	1	A_1	3430.6963	1	−9
6	1	A_2	3431.1333	3	−2
6	0	E	3431.2862	2	8
6	1	E	3430.9699	4	−5
6	2	A_1	3429.9971	2	8
6	2	A_2	3429.9692	5	2
6	3	E	3428.4331	2	−2
6	4	E	3426.0412	1	−6
6	5	A	3423.1388	5	−1

Table 2 (*continued*)

J	K	Γ	E	Δ	δ
1			2	3	4
6	6	E	3419.5589	3	4
7	7	A	3448.4822	12	−21
7	6	E	3452.3276	19	−29
7	5	E	3455.5515	−9	−5
7	4	A_1	3458.2059	10	−19
7	4	A_2	3458.2059	10	28
7	3	E	3460.3129	10	14
7	2	E	3461.8427	−5	6
7	1	A_1	3463.1893	3	−3
7	1	A_2	3462.6645	7	−9
7	0	E	3463.2857	1	4
7	1	E	3462.9562	12	−4
7	2	A_1	3461.9100	1	7
7	2	A_2	3461.9305	4	7
7	3	E	3460.4072	6	−3
7	4	E	3457.9306	8	−6
7	5	A	3455.0477	5	−7
7	6	E	3451.4747	5	5
7	7	E	3447.2361	11	6
8	8	E	3480.6535	8	−3
8	7	A	3485.1572	13	−13
8	6	E	3489.0033	10	−9
8	5	E	3492.2203	3	−12
8	4	A_1	3494.8433	2	9
8	4	A_2	3494.8554	3	−1
8	3	E	3496.8538	1	1
8	2	E	3498.3719	6	−3
8	1	A_1	3499.2283	2	−1
8	1	A_2	3499.8124	4	−14
8	0	E	3499.8579	10	0
8	1	E	3499.5181	2	−7
8	2	A_1	3498.3926	2	6
8	2	A_2	3498.4040	6	8
8	3	E	3496.9756	9	16
8	4	E	3494.3510	12	−2
8	5	A	3491.4983	2	−4
8	6	E	3487.9339	3	3
8	7	E	3483.7006	5	0
8	8	A	3478.8039	7	−16
9	9	E	3516.7265	7	1
9	8	E	3521.8965	3	−2
9	7	A	3526.3916	4	−4
9	6	E	3530.2306	8	−3
9	5	E	3533.4359	4	−9
9	4	A_1	3536.0494	3	8
9	4	A_2	3536.0173	6	9
9	3	E	3537.8935	3	−9
9	2	E	3539.4437	3	−7
9	1	A_1	3541.0001	5	−16
9	1	A_2	3540.3870	1	2
9	0	E	3541.0014	12	1
9	1	E	3540.6578	3	−4
9	2	A_1	3539.4470	5	3
9	2	A_2	3539.3749	10	6
9	3	E	3538.1331		58
9	4	E	3535.2934	6	−2
9	5	A	3532.4833	4	−6
9	6	E	3528.9322	10	7
9	7	E	3524.7081	2	6
9	8	A	3519.8206	9	8
9	9	E	3514.2670	6	−25
10	10	A	3556.7116	31	−22

Table 2 (*continued*)

J	K	Γ	E	Δ	δ
1			2	3	4
10	9	E	3562.5495	20	18
10	8	E	3567.6986	12	10
10	7	A	3572.1783	6	4
10	6	E	3576.0030	3	−3
10	5	E	3579.1892	9	−10
10	4	A_1	3581.7045	6	18
10	4	A_2	3581.7828	3	−4
10	2	E	3585.0521	12	−17
10	1	A_1	3586.1329	2	7
10	1	A_2	3586.7421		−57
10	0	E	3586.7114	10	−2
10	1	E	3586.3731	1	−2
10	2	A_1	3584.8747	6	−7
10	2	A_2	3585.0360	9	3
10	3	E	3583.8386	7	29
10	4	E	3580.7514	4	10
10	5	A_1	3577.9959	8	18
10	5	A_2	3577.9959	8	−7
10	6	E	3574.4623	6	3
10	7	E	3570.2515	3	0
10	8	A	3565.3760	2	−3
10	9	E	3559.8319	16	3
11	10	A	3607.1263	7	−33
11	9	E	3612.9370		86
11	8	E	3618.0567	9	57
11	7	A	3622.5105	5	11
11	6	E	3626.3126	13	−8
11	5	E	3629.4667		−49
11	4	A_1	3632.0462	5	−18
11	4	A_2	3631.8601		5
11	2	E	3635.1939		−14
11	1	A_2	3636.4531	3	8
11	0	E	3636.9828	2	−8
11	1	E	3636.6597	7	3
11	2	A_1	3635.1638	8	−11
11	2	A_2	3634.8951	10	−12
11	4	E	3630.7168	5	16
11	5	A_1	3628.0277	2	−25
11	5	A_2	3628.0277	2	34
11	6	E	3624.5203	5	1
11	7	E	3620.3276	9	−15
11	8	A	3615.4736	10	−3
12	10	A	3662.1141	8	19
12	9	E	3667.8651		0
12	7	A	3677.3834		45
12	6	E	3681.1505	10	−12
12	5	E	3684.2652	3	−10
12	4	A_1	3686.4336	12	24
12	4	A_2	3686.8299		−42
12	2	E	3689.8626	5	−26
12	1	A_1	3691.3352	9	0
12	1	A_2	3691.8902	8	−17
12	0	E	3691.8118	16	6
12	1	E	3691.5093	3	2
12	2	A_1	3689.4386	10	−1
12	2	A_2	3689.8304	5	6
12	4	E	3685.1846	4	11
12	5	A_1	3682.5730		60
12	5	A_2	3682.5730		−60
12	6	E	3679.1003	7	−12
12	7	E	3674.9366	7	−18
12	8	A	3670.1144	6	4
13	10	A	3721.6669	5	42
13	9	E	3727.3510	10	−54
13	4	A_1	3746.1305	6	9
13	4	A_2	3745.4006	2	49
13	2	E	3749.0568	11	−12
13	1	A_2	3750.7691	3	−6
13	0	E	3751.1888	9	18
13	1	E	3750.9135	8	0
13	2	A_1	3749.0235	1	−5
13	2	A_2	3748.5061	4	5
13	4	E	3744.1530	5	−17
13	5	A_1	3741.6264		−104
14	4	A_2	3809.9227		28
14	2	E	3812.7744	7	50
14	1	A_1	3814.7439	2	−10
14	0	E	3815.1035		0
14	1	E	3814.8632	8	1
14	2	A_1	3812.1049	7	−3
14	2	A_2	3812.7426	4	7
15	1	A_2	3883.2518	14	6
15	2	A_1	3880.9791	53	26
15	1	E	3883.3481	10	−5

[a] See footnote to Table 1.

5. Prediction of spectroscopic parameters by a local mode model

Although the isolated analysis of the upper rovibrational energies of the states $(2000, A_1)$ and $(1010, E)$ leads to an acceptable value of the *rms* deviations, unreasonable values of all centrifugal distortion parameters of both vibrational states are obtained.

Such a situation usually results from strong resonance interactions perturbing the rovibrational structure of the levels. In the present case both the $(2000, A_1)$ and $(1010, E)$ states of PD_3 can be perturbed by the (0020) A_1, and E states. However, not any transition of the $2\nu_3$ band was identified in the spectrum because the band is very weak.

An estimate of the main resonance interaction parameters and band centers of the $(0020, A_1)$ and $(0020, E)$ vibrational states is needed when the analysis is to be improved. For such an estimation, we assumed that the required vibrational energy values can be evaluated on the basis of the results of [20] which were shown to be valid for pyramidal XH_3-type molecules. Using Eqs. (45)–(50) of [20] the following relations are obtained:

$$\nu_1 = \omega + 2\lambda + 2x, \tag{14}$$

$$\nu_3 = \omega - 2\lambda + 2x, \tag{15}$$

$$\det \begin{vmatrix} 2\omega + 4\lambda + 14x/3 - E & F_0 = 2\sqrt{2}x/3 \\ 2\sqrt{2}x/3 & 2\omega - 4\lambda + 16x/3 - E \end{vmatrix} = 0, \tag{16}$$

and

$$\det\begin{vmatrix} 2\omega + 16x/3 - E & F_0 = 2\sqrt{2}x/3 \\ 2\sqrt{2}x/3 & 2\omega - 4\lambda + 14x/3 - E \end{vmatrix} = 0. \tag{17}$$

The first two relations provide directly the centers of the ν_1 and ν_3 bands. The solutions of the last two equations yield the band centers of $2\nu_1, A_1$, $2\nu_3, A_1$ and $\nu_1 + \nu_3, E$, $2\nu_3, E$ bands, respectively. Four experimental band centers are available: $\nu_1^{\text{exp.}} = 1682.12\,\text{cm}^{-1}$ and $\nu_3^{\text{exp.}} = 1693.35\,\text{cm}^{-1}$ from [15], $2\nu_1^{\text{exp.}} = 3332.54\,\text{cm}^{-1}$ and $\nu_1 + \nu_3^{\text{exp.}} = 3335.31\,\text{cm}^{-1}$ from the present work, Tables 1 and 2.

From these four values, three parameters were determined with the help of Eqs. (14)–(17) by a least squares fit procedure: $\omega = 1731.25\,\text{cm}^{-1}$, $x = -21.77\,\text{cm}^{-1}$ and $\lambda = -2.85\,\text{cm}^{-1}$. The parameters reproduce the band centers satisfactorily: $\nu_1^{\text{calc.}} = 1682.01\ \text{cm}^{-1}$, $\nu_3^{\text{calc.}} = 1693.41\,\text{cm}^{-1}$, $2\nu_1^{\text{calc.}} = 3332.71\,\text{cm}^{-1}$, and $(\nu_1 + \nu_3)^{\text{calc.}} = 3335.08\,\text{cm}^{-1}$. Such an agreement between the experimental and calculated values of the four band centers, with an *rms* deviation of $0.14\,\text{cm}^{-1}$ supports the conclusion that the two other band centers, namely $2\nu_3$, A_1, and $2\nu_3$, E, will be correctly predicted by Eqs. (16) and (17) from the parameters ω, x, and λ. The results are: $2\nu_3(A_1)^{\text{calc.}} = 3374.59\,\text{cm}^{-1}$ and $2\nu_3(E)^{\text{calc.}} = 3383.62\,\text{cm}^{-1}$. In addition, according to Eqs. (16) and (17), the predicted value of purely vibrational resonance parameters is $F_0 = -20.52\,\text{cm}^{-1}$ for interactions both between the states $(2000, A_1)/(0020, A_1)$ and $(1010, E)/(0020, E)$.

To estimate the "sensitivity" of the local mode formulas (14)–(17) to the real experimental band centers for PD_3 we have determined the three parameters ω, x, λ from three of the known band centers and then calculated the known fourth one thereof. Four such calculations were performed for the four different possibilities. In the worst case the difference $\Delta = \nu^{\text{calc.}} - \nu^{\text{exp.}}$ was $1.26\,\text{cm}^{-1}$. In this case the centers of the bands ν_1, $2\nu_1$ and $\nu_1 + \nu_3$ were used as initial data to calculate the center of the ν_3 band. The smallest absolute values of Δ were 0.46 and $0.42\,\text{cm}^{-1}$. All these results lead to the conclusion that the local mode approach is capable of estimating the wavenumbers of the doubly excited stretching states of PD_3, the unobserved "dark" states $2\nu_3, A_1$ and $2\nu_3, E$ included.

It should be mentioned that the parameter x of our model is nothing but the anharmonicity parameter for the P–D stretching mode. It can therefore be compared with the corresponding values of other related molecules. Such a comparison is possible with PH_2D for which x_{22} can be determined according to Eqs. (18) and (19) from ν_2 and $2\nu_2$:

$$\nu_2 = \omega_2 + x_{22} \tag{18}$$

and

$$2\nu_2 = 2\omega_2 + 4x_{22}. \tag{19}$$

The experimental band centers reported in Table 3 of [21] are $\nu_2 = 1688.512\,\text{cm}^{-1}$ and $2\nu_2 = 3333.673\,\text{cm}^{-1}$. Thereof we obtain $x_{22} = -21.676\,\text{cm}^{-1}$, which is close to the value for PD_3, $x = -21.77\,\text{cm}^{-1}$, derived in the present study.

6. Determination of spectroscopic parameters

For most of the light polyatomic molecules the rotational and centrifugal distortion parameters of stretching vibrational states differ only slightly from those of the ground vibrational state. Therefore values of the H and L sextic and octic centrifugal distortion coefficients of all four states under consideration, $(2000, A_1)$, $(0020, A_1)$, $(1010, E)$, and $(0020, E)$, treated in the fit were constrained to their ground state values reported in [17]. The starting values of the rotational and quartic centrifugal distortion parameters were linearly extrapolated from the values of the corresponding parameters in the ground state [17] and the states (1 0 0 0)/(0 0 1 0) [15].

The fit of "experimental" energies from Tables 1 and 2 was carried out with the mentioned constraints. Moreover, all the parameters of diagonal blocks, Eqs. (2) and (4), were kept fixed in the fit at the mentioned values with the exception of the rotational parameters and some of the quartic centrifugal distortion coefficients. The upper state energies, which were obtained from only one experimental transition and which are presented in Tables 1 and 2 without experimental uncertainties Δ, were not considered in the fit. No transitions belonging to the $2\nu_3, A_1/E$ band system could be assigned with confidence.

The 44 parameters derived from the analysis are presented in Tables 3 and 4 together with their 1σ statistical confidence intervals. These comprise 29 parameters belonging to the diagonal blocks and 15 which are interaction parameters. They reproduce the initial 305 upper experimental energies used in the fit, $J^{\max.} = 15$, with an *rms* deviation of $0.0015\,\text{cm}^{-1}$. The parameters of diagonal blocks given without confidence intervals were fixed as mentioned above. In column 4 of Tables 1 and 2 the values δ, in units of $10^{-4}\,\text{cm}^{-1}$, of the differences between experimental upper energies and the corresponding values calculated with the parameters gathered in Tables 3 and 4 are listed.

Inspection of the results evidences that the reproduction of the observations worsens as J exceeds 10. This feature can be ascribed to the effects of resonance interactions between the (2 0 0 0) and (1 0 1 0) states , on the one hand, and the (1 0 0 2) and (0 0 1 2) states, on the other hand. In our model the influence of the (1 0 0 2) and (0 0 1 2) (and further) states on the rovibrational

Table 3
Parameters of diagonal blocks of PD_3 (in cm^{-1})[a]

Parameter	$(2000, A_1)$	$(1010, E)$	$(0020, A_1)$	$(0020, E)$
E	3348.987814(841)	3346.718682(504)	3358.1426[d]	3372.2099[d]
B	2.304584(971)	2.262689(631)	2.285182352[b]	2.285182352[b]
C	1.9423605(534)	1.9475647(652)	1.957474765[b]	1.957474765[b]
$D_J \times 10^4$	0.23236(943)	0.21331(570)	0.33938219[b]	0.33938219[b]
$D_{JK} \times 10^4$	−0.38737026[b]	−0.41669426[b]	−0.44601826[b]	−0.44601826[b]
$D_K \times 10^4$	0.3064077[b]	0.3341147[b]	0.3618217[b]	0.3618217[b]
$H_J \times 10^8$	0.1387262[c]	0.1387262[c]	0.1387262[c]	0.1387262[c]
$H_{JK} \times 10^8$	−0.275063[c]	−0.275063[c]	−0.275063[c]	−0.275063[c]
$H_{KJ} \times 10^8$	0.199415[c]	0.199415[c]	0.199415[c]	0.199415[c]
$H_K \times 10^8$	0.04167[c]	0.04167[c]	0.04167[c]	0.04167[c]
$L_J \times 10^{13}$	−0.69831[c]	−0.69831[c]	−0.69831[c]	−0.69831[c]
$L_{JJK} \times 10^{13}$	0.7390[c]	0.7390[c]	0.7390[c]	0.7390[c]
$\epsilon' \times 10^5$	0.749235[c]	0.749235[c]	0.749235[c]	0.749235[c]
$\epsilon'_J \times 10^9$	−0.82353[c]	−0.82353[c]	−0.82353[c]	−0.82353[c]
$\epsilon'_K \times 10^9$	0.49104[c]	0.49104[c]	0.49104[c]	0.49104[c]

Parameter	$(1010, E)$	$(0020, E)$	Parameter	$(1010, E)$	$(0020, E))$
$2C\zeta$	0.059689(362)	0.085[e]	$\beta_J \times 10^4$	−0.0898(328)	
$\eta_J \times 10^3$	−0.1626(127)		$\beta_K \times 10^4$	1.970(199)	
$\eta_K \times 10^3$	0.1817(158)		$\beta_{JK} \times 10^6$	−0.1134(199)	
$\eta_{JJ} \times 10^6$	1.914(117)		$\gamma \times 10^2$	−0.53300(681)	
$\eta_{JK} \times 10^6$	−4.932(656)		$\gamma_K \times 10^4$	0.1913(162)	
$\eta_{KK} \times 10^6$	3.966(447)		$\gamma_{KK} \times 10^6$	0.5554(193)	
$\eta_{JJK} \times 10^8$	−2.407(264)		$\kappa \times 10^5$	−0.6575(480)	
$\alpha \times 10^2$	0.0902(180)		$\kappa_J \times 10^7$	0.1476(210)	
$\alpha_K \times 10^3$	0.9439(963)		$\kappa_K \times 10^7$	6.331(575)	
$\alpha_{KK} \times 10^4$	0.1426(137)		$\kappa_{JK} \times 10^9$	−2.474(254)	
$\beta \times 10^2$	0.5372(184)				

[a] Values in parentheses are 1σ statistical confidence intervals in units of the last digit.
[b] Extrapolated from the values of corresponding parameters of the (0000) [16], (1000) [15], and (0010) [15] vibrational states.
[c] Fixed to the value of corresponding parameter of the ground vibrational state [16].
[d] Fixed to the value estimated from the local mode model (see text for details).
[e] Fixed to the value of corresponding parameter for the (1010) state multiplied by $\sqrt{2}$.

energies of the (2000) and (1010) states was not taken into account. In addition, no transitions belonging to the $\nu_1 + 2\nu_4$ or $\nu_3 + 2\nu_4$ bands were identified. Nevertheless the achieved quality of the fit is satisfactory.

A table of the assigned allowed transitions together with the corresponding observed–calculated values derived from the parameters of Tables 3 and 4, can be obtained from IDEAL [22].

7. Are the (2000) and (1010) states of PD_3 local mode states?

Hydrides of the heavier elements of the fifth group of the periodic table, for example AsH_3 and SbH_3 [23,24], reveal local mode behavior already at low stretching vibrational excitation. As it was discussed in [1,2,25,26], for PH_3 and its deuterated isotopomers PH_2D and PHD_2, local mode behavior for the P–H stretching motion was established. One may expect that the spectroscopic properties of PD_3 may also behave to a certain extent according to the local mode model.

Inspection of the assignment of the spectrum and furthermore the fit of the upper rovibrational energies

Table 4
Parameters of resonance interactions of PD_3 (in cm^{-1})[a]

Parameter	Value
$(2000, A_1)/(0020, A_1)$ *Interaction*	
F_0	−20.52[b]
$F_{JKK} \times 10^6$	0.1702(111)
$F_J \times 10^2$	−0.9573(733)
$F_{JJJJ} \times 10^9$	−0.01677(426)
$F_{JJK} \times 10^6$	−0.13020(977)
$F_{JJJK} \times 10^9$	1.004(355)
$(1010, E)/(0020, E)$ *Interaction*	
F_0	−20.52[b]
$F_{JKK} \times 10^6$	0.2469(195)
$F_J \times 10^2$	1.8300(559)
$F_{JJJK} \times 10^9$	1.4133(608)
$F_{JJK} \times 10^6$	−0.2087(191)
$(2000, A_1)/(1010, E)$ *Interaction*	
$\alpha^* \times 10$	−0.6500(211)
$\beta^* \times 10^2$	0.4818(284)
$\alpha^*_J \times 10^4$	−0.3534(508)
$\gamma^* \times 10^2$	−0.78021(407)
$\alpha^*_{JJ} \times 10^7$	1.161(191)
$\gamma^*_J \times 10^6$	0.845(168)

[a] Values in parentheses are the 1σ statistical confidence intervals in units of the last digit.
[b] Fixed to the value estimated from the local mode model (see text for details).

allows one to draw conclusions about the closeness to the local mode limit of the PD_3 molecule in the (2 0 0 0) and (1 0 1 0) states. The analysis of the values of the band centers reported in the previous section indicates that the local mode model according to [20] is rather suitable for the description of the PD_3 stretching vibrational structure. The differences between the lowest energy vibrational stretching term values in the polyads $v = v_1 + v_3$ decrease with increasing v, e.g., from $11.17\,\mathrm{cm}^{-1}$ for $v = 1$ to $2.77\,\mathrm{cm}^{-1}$ for $v = 2$ in the $2v_1/v_1 + v_3$ pair but it is still substantial rather than zero.

Likewise the values of the main Coriolis type interaction parameters, $(C\zeta_z)$ and $(B\zeta_x)$, also decrease with v from $C\zeta_z = 0.1095\,\mathrm{cm}^{-1}$ in the v_3 band [15] to $0.0298\,\mathrm{cm}^{-1}$ in the $v_1 + v_3$ band and the $(B\zeta_x)$[2] resonance interaction parameter from $0.0549\,\mathrm{cm}^{-1}$ in the v_1/v_3 pair [15] to $0.06500/\sqrt{2} = 0.04596\,\mathrm{cm}^{-1}$ in $2v_1/v_1 + v_3$. However, both $C\zeta_z$ and $B\zeta_x$ are still significantly away from zero as demanded for a fully local mode stretching state. Finally, it is a feature of local mode states that they are decoupled from other states involving multiply excited bending states. The substantial intensity of the $v_1 + 2v_4/v_3 + 2v_4$ bands, see Fig. 1, is in contradiction to this expectation. We thus conclude that, although the $2v_1$ and $v_1 + v_3$ overtone levels of PD_3 have much in common with typical local mode states ($(200A_1/E)$ in the local mode notation), these states have not yet reached true local mode behavior.

8. Conclusion

The high resolution infrared spectrum of PD_3 has been studied for the first time in the region of the first stretching overtone bands. The analysis of the $2v_1$ and $v_1 + v_3$ bands identified in the spectrum revealed that in addition to the Coriolis interactions between them perturbations both by the stretch-bend combination states $v_1 + 2v_4/v_3 + 2v_4$ and the stretching overtone $2v_3$, A_1/E are present. Although the (2 0 0 0) and (1 0 1 0) states have not yet reached the local mode limit they reveal features which can be successfully modelled using the local mode concept. The 305 upper "experimental" rovibrational energies of the (1 0 1 0) and (2 0 0 0) states can be reproduced with a *rms* deviation of $0.0015\,\mathrm{cm}^{-1}$ using in total 44 refined Hamiltonian parameters.

[2] The following relation is valid: $(B\zeta_x) = C_{11}^{(1)} = -\alpha^* v_1^{-1/2}$. Here the α^* and $C_{11}^{(1)}$ are the Coriolis interaction parameters in notations of the present contribution and of [15], respectively.

Acknowledgment

We thank the Deutsche Forschungsgemeinschaft for financial support.

References

[1] O.N. Ulenikov, E.S. Bekhtereva, O.L. Petrunina, H. Bürger, W. Jerzembeck, J. Mol. Spectrosc. 219 (2003) 13–29.
[2] O.N. Ulenikov, O.L. Petrunina, E.S. Bekhtereva, E.A. Sinitsin, H. Bürger, W. Jerzembeck, J. Mol. Spectrosc. 215 (2002) 85–92.
[3] A.T. Tokunaga, R.F. Knacke, S.T. Ridgway, L. Wallace, Astrophys. J. 232 (1979) 603–615.
[4] R.F. Knacke, S.J. Kim, S.T. Ridgway, A.T. Tokunaga, Astrophys. J. 262 (1982) 388–395.
[5] L.-M. Lara, B. Bezard, C.A. Griffitth, J.H. Lacy, T. Owen, ICARUS 131 (1988) 317–333.
[6] C. Camy-Peyret, J.-M. Flaud, A. N'Gom, J.W.C. Johns, Mol. Phys. 65 (2002) 649–657.
[7] O.N. Ulenikov, R.N. Tolchenov, E.N. Melekhina, M. Koivusaari, S. Alanko, R. Anttila, J. Mol. Spectrosc. 170 (1995) 397–416.
[8] O.N. Ulenikov, G.A. Onopenko, N.E. Tyabaeva, H. Bürger, W. Jerzembeck, J. Mol. Spectrosc. 197 (1999) 100–113.
[9] H. Qian, Q.-S. Zhu, H. Ma, B.A. Thrush, Chem. Phys. Lett. 192 (1992) 338–347.
[10] H.W. Kattenberg, A. Oskam, J. Mol. Spectrosc. 49 (1974) 52–69.
[11] H.W. Kattenberg, R. Elst, A. Oskam, J. Mol. Spectrosc. 47 (1973) 55–63.
[12] G. Pierre, V. Boudon, E.B. Mkadmi, H. Bürger, D. Bermejo, R. Martinez, J. Mol. Spectrosc. 216 (2002) 408–418.
[13] M. Halonen, L. Halonen, H. Bürger, W. Jerzembeck, J. Chem. Phys. 108 (1998) 9285–9290.
[14] K. Kijima, T. Tanaka, J. Mol. Spectrosc. 89 (1981) 62–75.
[15] E. Canè, L. Fusina, W. Jerzembeck, H. Bürger, J. Mol. Spectrosc. 220 (2003) 242–247.
[16] E. Canè, L. Fusina, W. Jerzembeck, H. Bürger, J. Mol. Spectrosc. 218 (2003) 28–35.
[17] E. Canè, L. Fusina, H. Bürger, W. Jerzembeck, S. Brünken, F. Lewen, G. Winnewisser, J. Mol. Spectrosc. 215 (2002) 1–9.
[18] R.A. Toth, J. Opt. Soc. Am. B 10 (1993) 2006–2029.
[19] O.N. Ulenikov, A.B. Malikova, S. Alanko, M. Koivusaari, R. Anttila, J. Mol. Spectrosc. 179 (1996) 175–194.
[20] I.M. Mills, A.G. Robiette, Mol. Phys. 56 (1985) 743–765.
[21] O.N. Ulenikov, O.L. Khabibulina, E.S. Bekhtereva, H. Bürger, W. Jerzembeck, J. Mol. Spectrosc. 217 (2003) 288–297.
[22] Supplementary data for this article are available on IDEAL (http://www.idealibrary.com) and as a part of the Ohio State University Molecular Spectroscopy Archives (http://msa.lib.ohio-state.edu/jmsa hp.htm).
[23] M. Halonen, L. Halonen, H. Bürger, P. Moritz, J. Chem. Phys. 95 (1991) 7099–7107.
[24] M. Halonen, L. Halonen, H. Bürger, P. Moritz, J. Phys. Chem. 96 (1992) 4225–4231.
[25] O.N. Ulenikov, H. Bürger, W. Jerzembeck, G.A. Onopenko, E.S. Bekhtereva, E.A. Sinitsin, J. Mol. Spectrosc. 208 (2001) 236–248.
[26] O.N. Ulenikov, E.S. Bekhtereva, T.D. Homiak, T.R. Huet, F. Herregodts, H. Bürger, W. Jerzembeck, J. Mol. Spectrosc., in press.